SAND2022-10384C

Sandia National Laboratories

Algorithms for Handling Low-density Plasmas in PERSEUS with Tabular Material Models

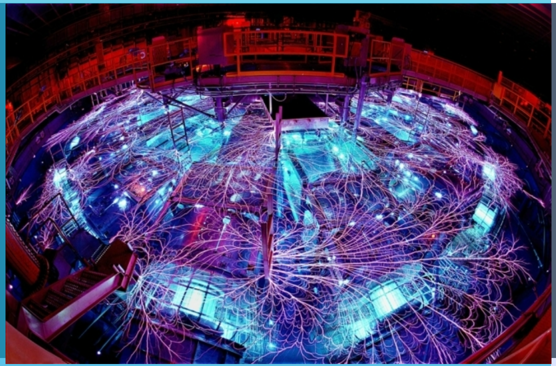

PRESENTED BY

Nathaniel D. Hamlin, Matthew R. Martin

This work is supported by the National Nuclear Security Administration stewardship sciences academic program under Department of Energy cooperative agreements DE-FOA-0003764, DE-FOA-0001153 and DE-NA0001836.

SAND number:

Sandia National Laboratories is a multimission laboratory managed and operated by National Technology & Engineering Solutions of Sandia, LLC, a wholly owned subsidiary of Honeywell International Inc., for the U.S. Department of Energy's National Nuclear Security Administration under contract DE-NA0003525.

Sandia National Laboratories is a multimission laboratory managed and operated by National Technology & Engineering Solutions of Sandia, LLC, a wholly owned subsidiary of Honeywell International Inc., for the U.S. Department of Energy's National Nuclear Security Administration under contract DE-NA0003525.

Outline

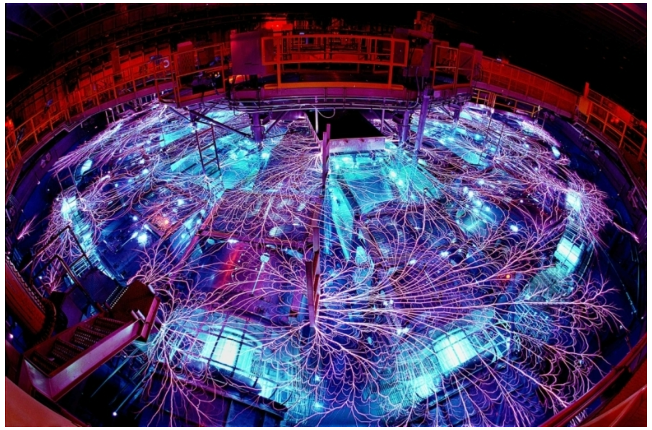

- Overview of numerical methods in PERSEUS:
  - GOL with electron inertia and displacement current (PERSEUS/FLEXO) versus MQS approximation (Hydra)
  - Tabular EOS/conductivity interface in PERSEUS
  - Vacuum/floor treatment
  - Modifications to SESAME EOS and conductivity tables
- 1D liner simulations
  - Influence of Hall term on floor convergence of post-stagnation dynamics
  - Reduced sensitivity to other vacuum parameters at sufficiently low density floors
  - PERSEUS vacuum modeling convergence study: with vs without Hall term
- 2D MRT simulations
  - Cu MRT is converged w.r.t. density floor, and shows minimal sensitivity to vacuum parameters.
  - Cu MRT shows reduced growth rates at higher floors, e.g. 1e-6 of solid.
  - Sinusoidal outer surface: recovery of analytic linear MRT growth rates.
- 1D Cu slab tabular validation problem
  - Cross-validation of tabular interface between PERSEUS and FLEXO

What are PERSEUS and FLEXO?

- PERSEUS (Plasma as an Extended-MHD Relaxation System with an Efficient Upwind Scheme):
  - Extended-MHD code originally developed by Matt Martin and Charles Seyler at Cornell University, and under continued development at Sandia.
  - Models larger range of plasma densities than previously feasible.
  - Captures interactions with low-density plasma: more predictive modeling of target performance in a pulsed-power device.
- FLEXO (Flux-Limited Extended Ohm's Law):
  - Next-generation production-line version of PERSEUS, currently under development at Sandia.
  - Everything PERSEUS has, plus:
    - Adaptive Mesh Refinement (AMR) to resolve spatial details, e.g. stagnation column, small-wavelength modes.
    - Multi-material modeling
    - Portability between different architectures, e.g. CPUs and GPUs.

PERSEUS/FLEXO Can Model Experimental Vacuum Conditions

- Experimental vacuum pressure of 10^{-5} Torr on Z corresponds to densities 10 to 12 orders of magnitude below solid density!
- This density range has, until now, been numerically intractable.
  - Due to unbounded phase velocity becoming prohibitively large at vacuum densities.
  - Plasma-vacuum interface problem has plagued pulsed-power calculations for more than two decades!
- PERSEUS/FLEXO extended-MHD model overcomes this challenge.
  - Displacement current included: phase velocities bounded by numerical speed of light.
  - More predictive model of current coupling onto target: models current carried by low-density plasma.
  - Reduced sensitivity to parameters characterizing numerical vacuum.

Direct numerical simulation of the plasma vacuum interface problem in XMHD

- The plasma-vacuum interface problem has plagued pulsed power calculations for more than two decades
- The experimental initial conditions on the Z facility includes near solid metal density liners with current carried through electrodes separated by a 1E-5 torr gas density
- This density variation of 1E-10 to 1E-12 was intractable to directly simulate until the development of the XMHD PERSEUS and FLEXO codes due to the unbounded phase velocity of the discretized equations in previous codes
- The following slides describe a resolution of this floor problem in XMHD through direct numerical simulation of the full density range found in experiments and how this treatment removes the sensitivities seen in typical calculations where only up to 1E-6 density variation in the floors is computationally feasible in MHD

Comparison of timestep scaling in PERSEUS(EMEI-XMHD) and HYDRA(ALE MHD or Hall MHD) with density

- $\Delta t = CFL * \frac{\Delta x}{v}$
- Δt limited by Alfven speed when displacement current is omitted:
  - PERSEUS (GOL with displacement current): $v_A \sim \frac{B^2(\mu_0\rho)^{-1}}{\sqrt{1+B^2(\mu_0\rho c^2)^{-1}}} \leq c$
  - Magneto-quasistatic (MQS) GOL: $v_A \sim \frac{B}{\sqrt{\mu_0\rho}}$ is unbounded as $\rho \to 0$.
- Whistler wave introduced by Hall term: $\Omega_{whistler} \sim kv_A(1 + k\lambda_i)$
  - Does not need to be resolved with PERSEUS semi-implicit GOL formulation.
- In PERSEUS, only sources are implicit, so the solve is local.
  - Avoids CPU expense of global solves.
  - Current density is time-advanced in GOL: avoids numerical precision issues with computing current in dense plasma (adding charge-to-mass-weighted ion and electron momenta).
- Semi-implicit advance with Hall and displacement current is implemented in FLEXO, and appears to be working:
  - FLEXO correctly models a 1-D Whistler wave using Hall physics.

Other aspects of PERSEUS and FLEXO implementation

- Tabular interface:
  - tabular EOS: $P(\rho, T)$, $\epsilon_{int}(\rho, T)$
  - tabular conductivity: $\sigma(\rho, T)$, $Z_{eff}(\rho, T)$, $\kappa(\rho, T)$
  - PERSEUS loads tables at start of simulation.
  - Interpolation during simulation:
    - Reverse-interpolate to compute T from ρ and E_{int} .
    - Interpolate to compute $\mathrm{X}(\rho, T)$ from ρ and T.
  - Interfaces with C-routines provided by Kyle Cochrane.
- Discontinuous Galerkin (DG) spatial discretization:
  - Spectral method that models spatial variation within each cell.
- Positivity-preserving limiting on density and internal energy.
  - Adjust slopes so that if cell-centered values are above the floor, all nodal values in cell are above the floor.
- Parallelization through Message-Passing Interface (MPI).
- FLEXO also has:
  - Adaptive Mesh Refinement (AMR) to resolve spatial details, e.g. stagnation column, small-wavelength modes.
  - Multi-material modeling
  - Portability between different architectures, e.g. CPUs and GPUs.

At sufficiently low density floors, PERSEUS with Hall MHD shows little sensitivity to the floor multiplier or to floor resets (shown in 1-D liner results).

SESAME EOS and conductivity table modifications required for this modeling approach

- HYDRA and PERSEUS currently use different tables.
- Tables extended to lower densities (by Kyle Cochrane) to allow lower vacuum densities.
- Tension regime $(P < 0)$ replaced with Maxwell constructions (by John Carpenter) in vapor dome to avoid negative pressures.
  - PERSEUS is not currently doing material strength modeling.

Tension regime (Cu 3325)

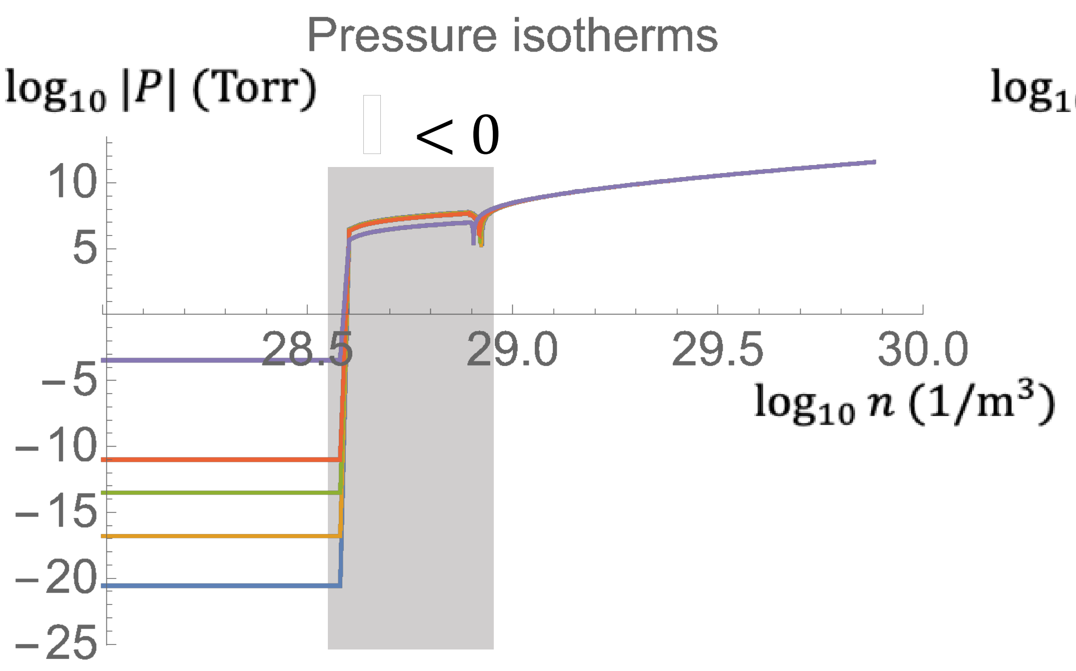

Maxwell constructions (Cu 3326)

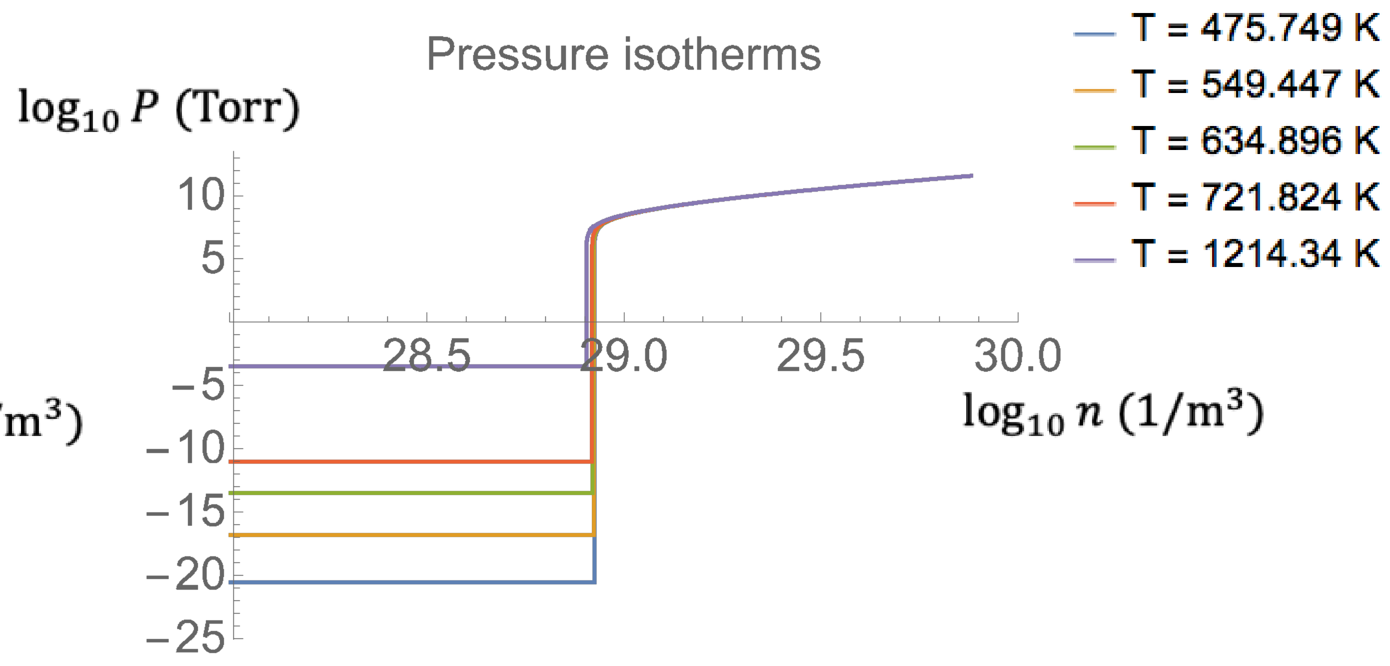

1-D Cu liner implosion problem

- Radially convergent cylindrical geometry
- Aspect ratio = 6
- Initial density = 8900 kg/m^3 (Cu)
- Initial temperature = 1130 K
- Initial pressure ~ 5×10^{-5} Torr
- Cu with Maxwell constructions (Cu 3326)
- Peak current = 26 MA
- $I(r_{max}, t) = I_{max}\sin^2\left(\frac{\pi t}{2\tau}\right)$
- t_final = 2*t_rise $= 2\tau$
- 100-ns rise time:
  - Domain: $\mathrm{r} = 0$ to $\mathrm{r} = 8$ mm, 400 cells
  - Outer radius = 1.92 mm
  - Inner radius = 1.6 mm
- 10-ns rise time:
  - Domain: $\mathrm{r} = 0$ to $\mathrm{r} = 8/\sqrt{10}$ mm, 400 cells
  - Outer radius = $1.92/\sqrt{10}$ mm
  - Inner radius = $1.6/\sqrt{10}$ mm

$$\Pi = \frac{\mu_0 I_{max}^2 \tau^2}{4\pi m_{hat} r_o^2} = 5.8$$

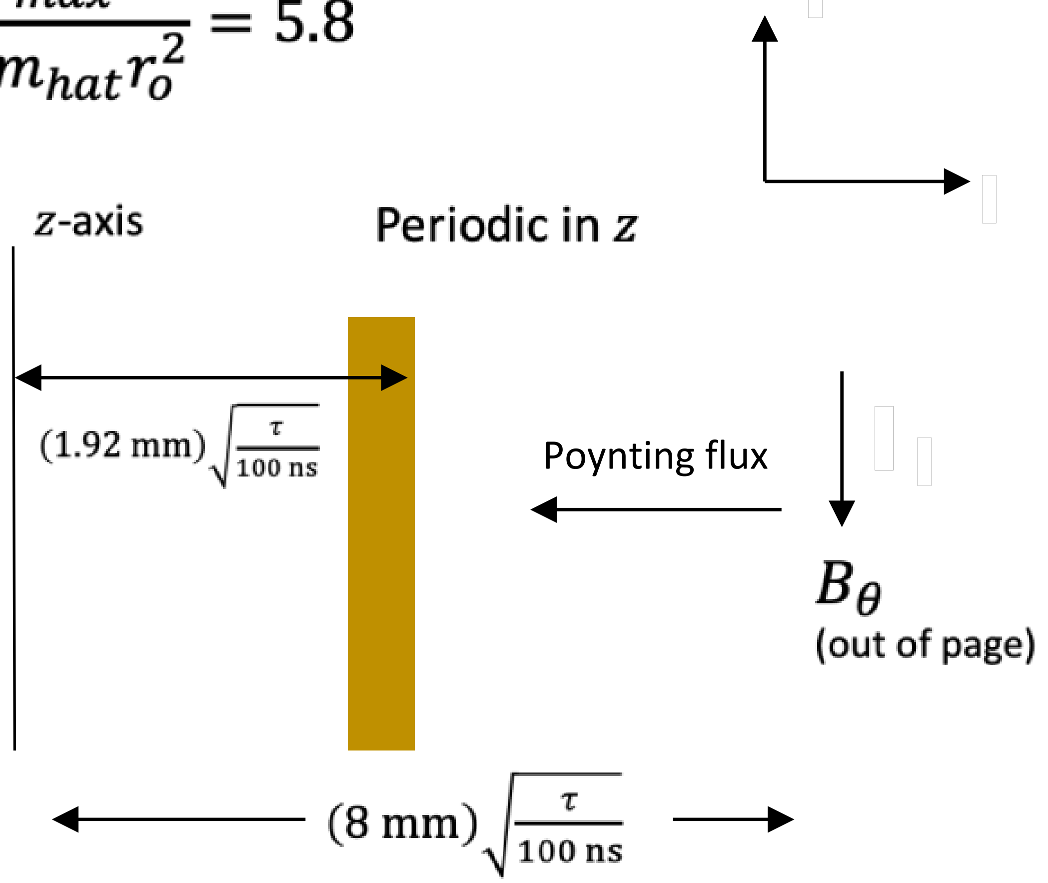

Extended-MHD in a 1-D liner: with vs without Hall term

t_rise = 10 ns

Outer radius = $\frac{1.92}{\sqrt{10}}$ mm

$\Delta r = \frac{1.92}{6\sqrt{10}} = 0.10$ mm

Cylindrical liner
26 MA peak current
AR = 6

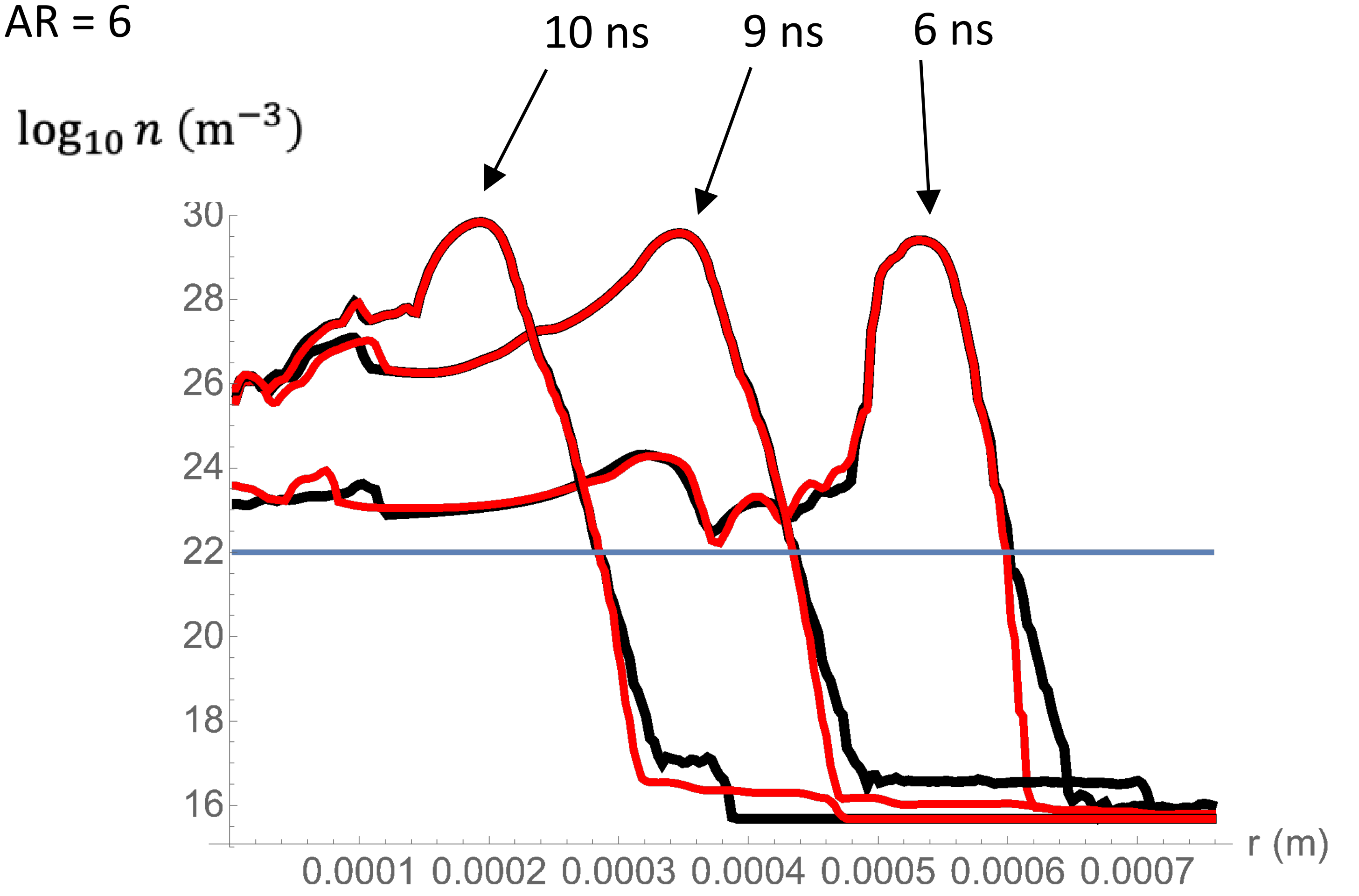

1-D bulk implosion dynamics show little sensitivity to Hall term.

- Sensitivity emerges at low densities.
- For 1-D implosion, Hall sensitivity emerges in post-stagnation.

Cylindrical liner
26 MA peak current
100-ns rise time

AR = 6
1.92-mm outer radius
1 mg/cc gas fill
Floor multiplier = 4
Implosion phase converged

Faster convergence in post-stagnation when Hall term is included.

Hall EMEI-MHD

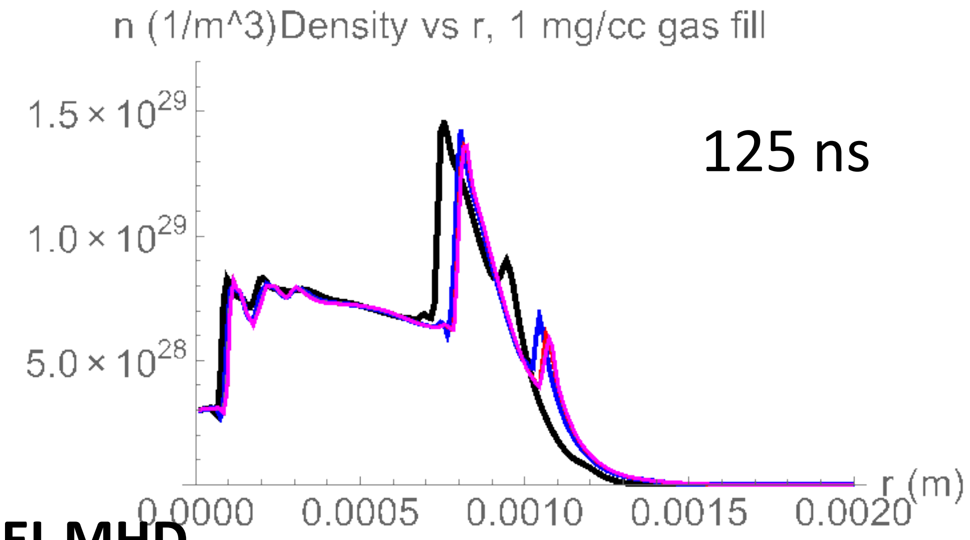

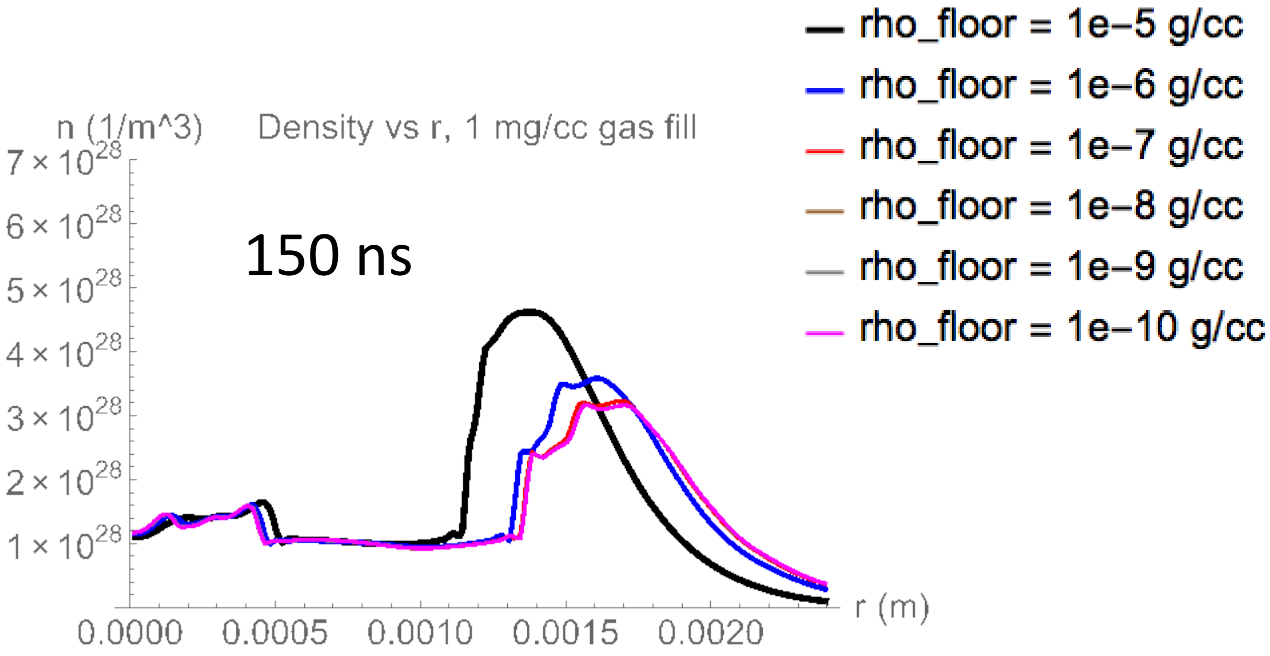

EMEI-MHD

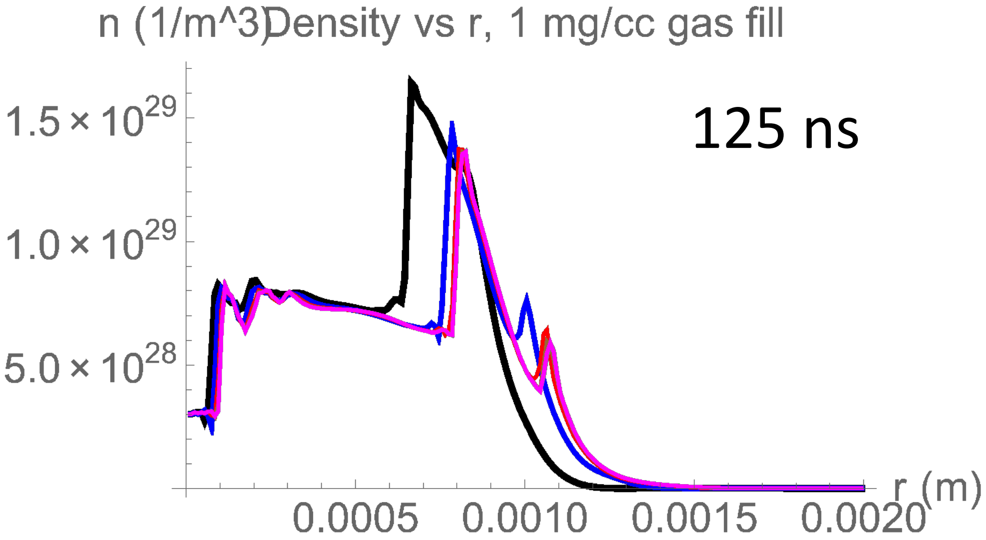

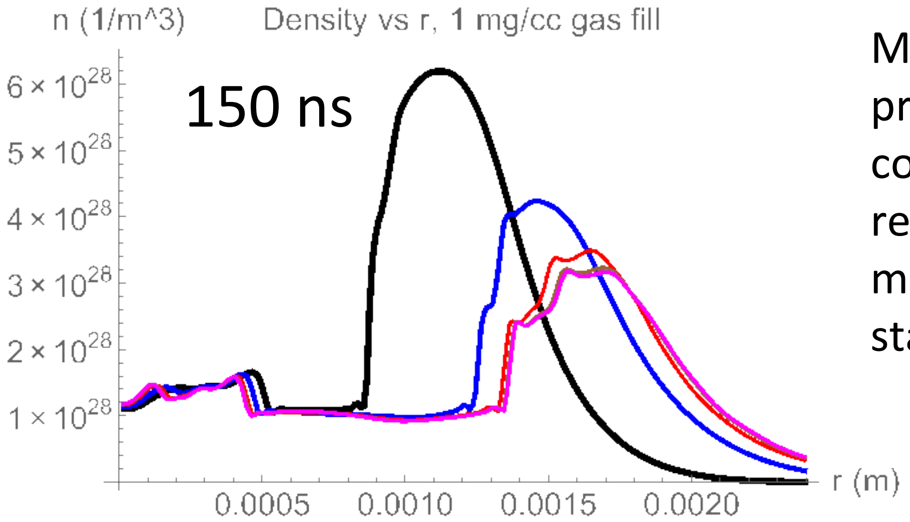

More accurate prediction of confinement times requires accurate modeling of post-stagnation.

Cylindrical liner
26 MA peak current
100-ns rise time
SOL = c/30

AR = 6
1.92-mm outer radius
1 mg/cc gas fill
Implosion phase converged

At sufficiently low density floors, post-stagnation has minimal sensitivity to the floor multiplier.

Floor multiplier: reset of momentum and energy for $\rho \leq \rho_{multiplier}\rho_{floor}$.

Hall EMEI-MHD

150 ns

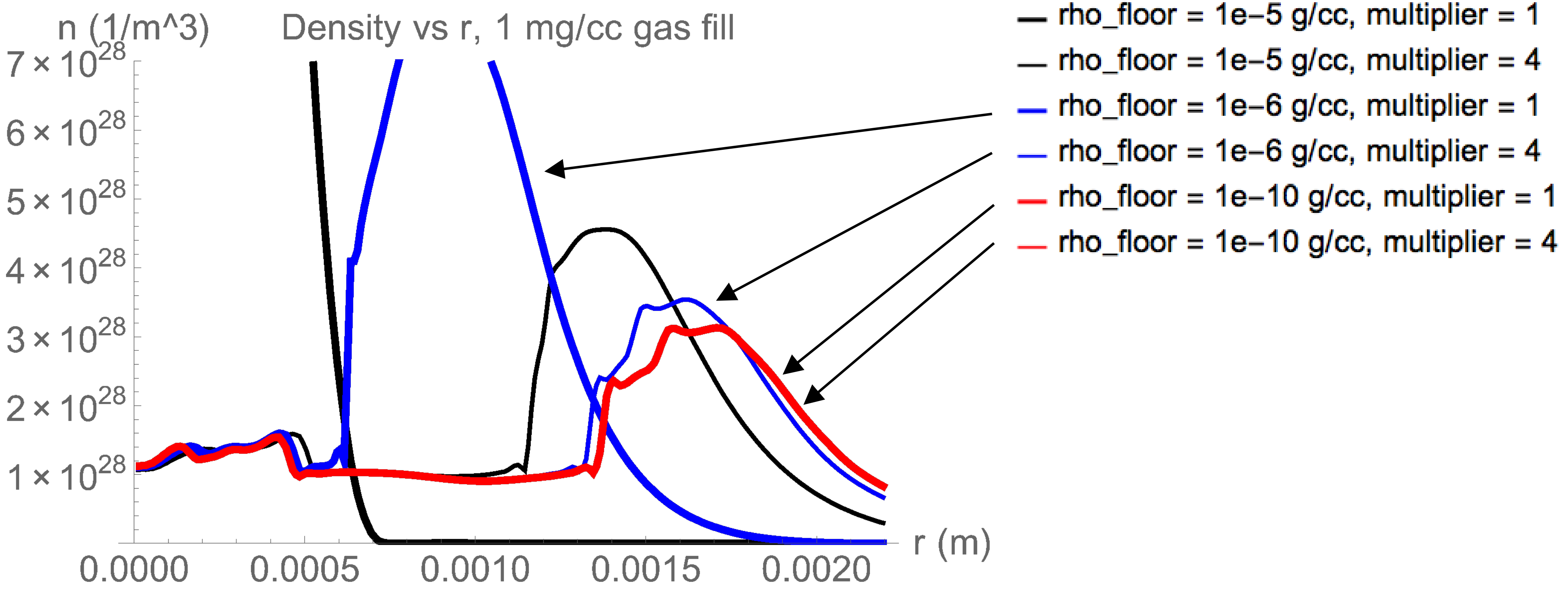

Cylindrical liner	AR = 6
26 MA peak current	1.92-mm outer radius
100-ns rise time	1 mg/cc gas fill
SOL = c/30	

At sufficiently low density floors, post-stagnation has minimal sensitivity to the use of a pressure floor.

Pressure floor: Optional reset of computed pressure to floor value if less than floor value.

Hall EMEI-MHD 150 ns

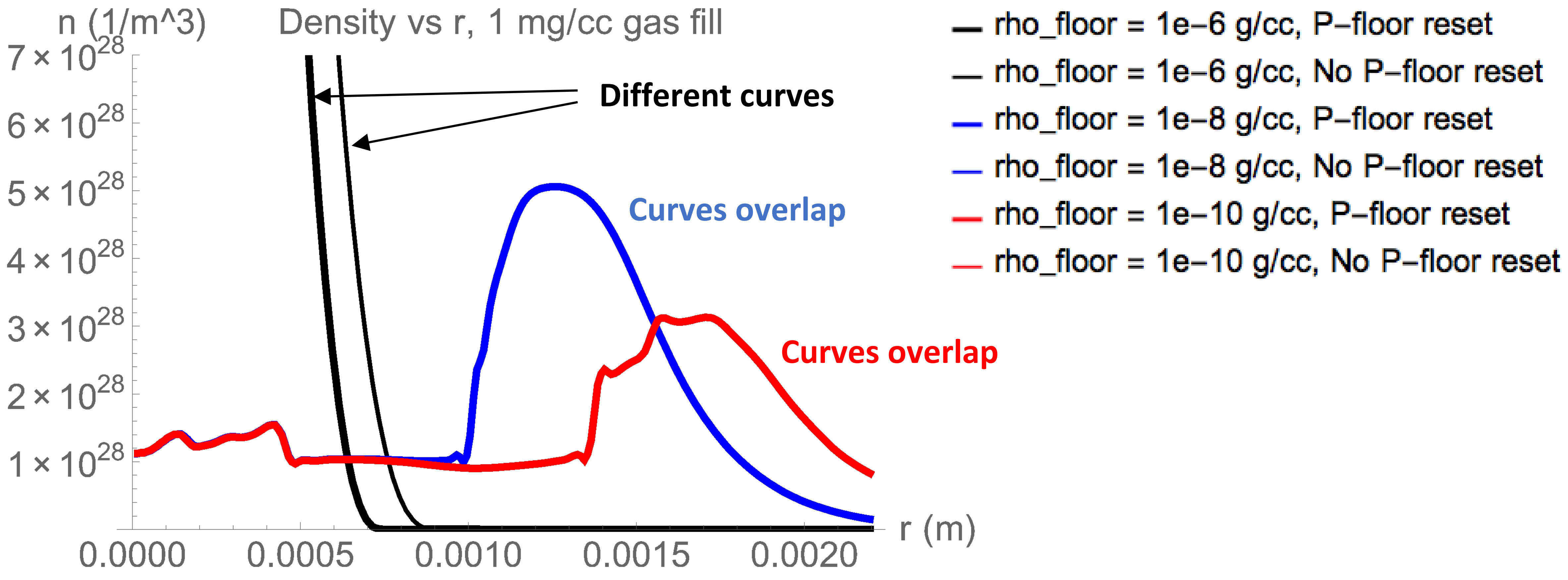

2-D MRT problem

- Axisymmetric cylindrical geometry
- Initial temperature = 1130 K for Cu
- Initial pressure ~ 5×10^{-5} Torr
- Peak current = 26 MA
- $I(r_{max}, t) = I_{max}\sin^2\left(\frac{\pi t}{2\tau}\right)$
- 100-ns rise time:
- Domain: 3.84x2.4 mm, 192x120 cells
- Cell size = 20 microns
- Cu Liner Parameters:
  - Initial density = 8960 kg/m^3
  - Aspect ratio = 32
  - Outer radius = 2.88 mm
  - Inner radius = 2.79 mm
  - Same Π-parameter as Be with AR = 6
- MRT seed:
  - 1% sinusoidal temperature perturbation in outer layer of cells on liner surface.
  - λ = 200 microns

$$\Pi = \frac{\mu_0 I_{max}^2 \tau^2}{4\pi m_{hat} r_o^2} = 5.7$$

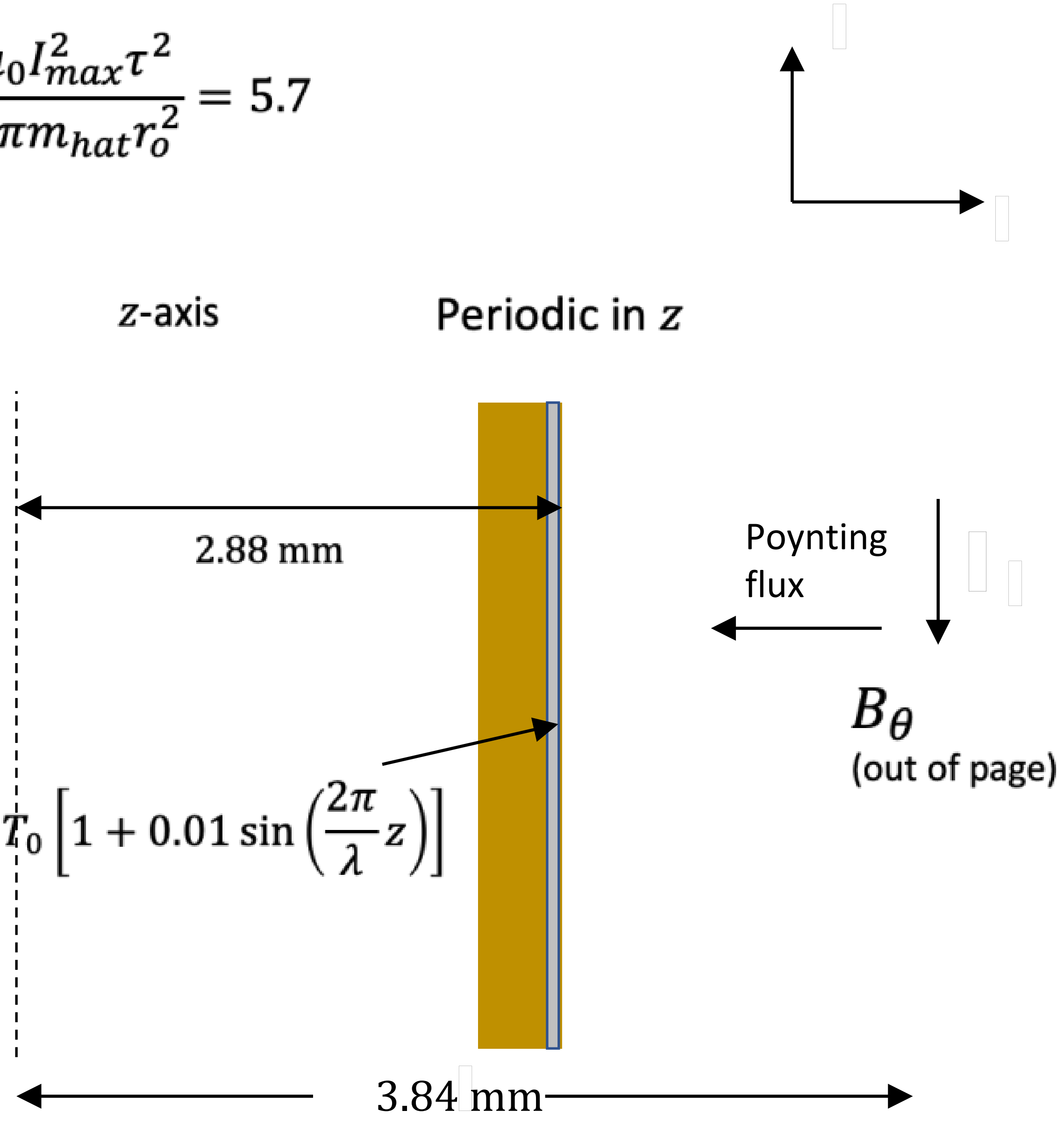

$$T(z) = T_0\left[1 + 0.01\sin\left(\frac{2\pi}{\lambda}z\right)\right]$$

At sufficiently low density floors, 2D MRT development is converged, and shows minimal dependence on temperature and pressure floor resets.

Copper

XMHD, 10^{-11} density floor, P and T-floor resets	XMHD, 10^{-10} density floor, P and T-floor resets	XMHD, 10^{-11} density floor, No P and T-floor resets	XMHD, 10^{-10} density floor, No P and T-floor resets

Rows: 80 ns, 90 ns, 100 ns

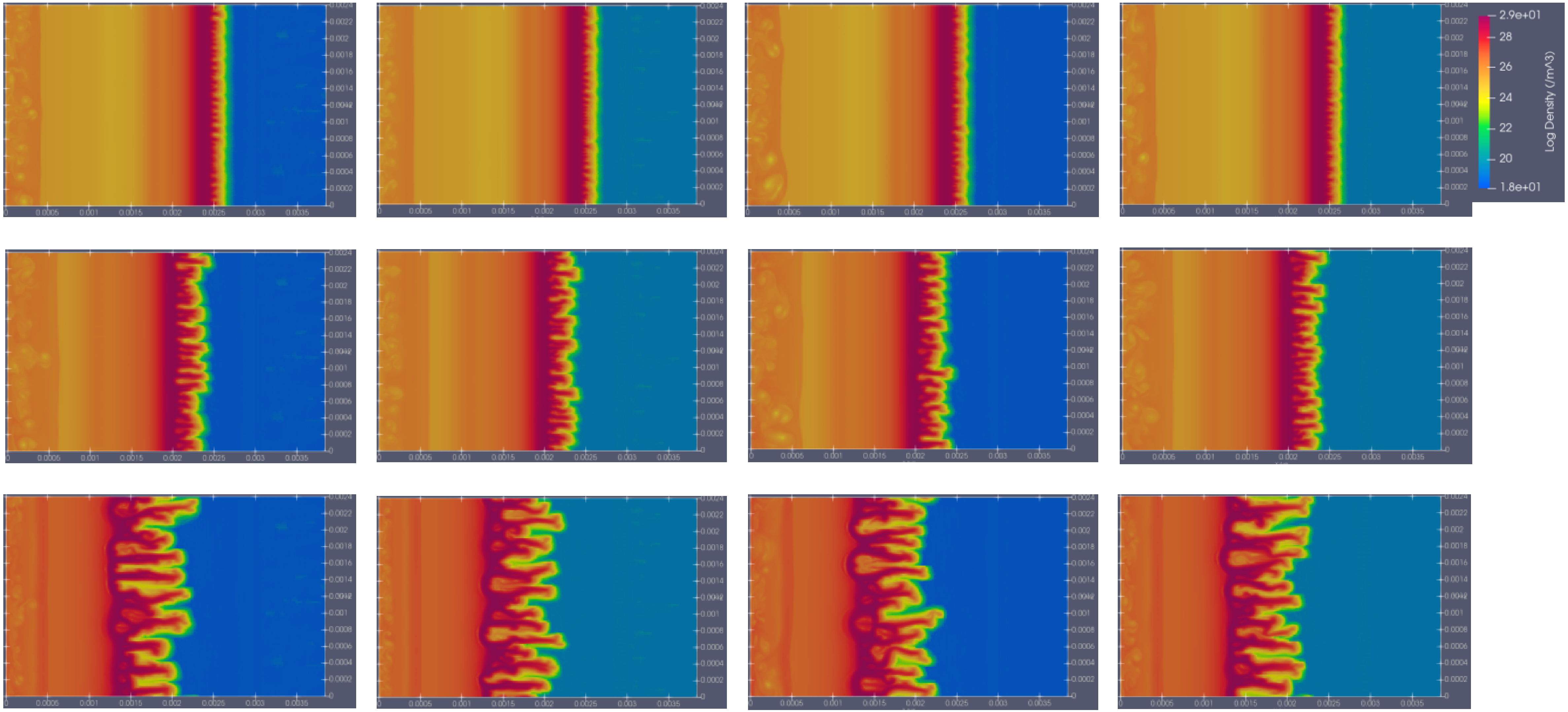

Higher density floors give slower MRT growth rates; not converged.

Copper

XMHD, 10^{-10} density floor P and T-floor resets	EMEI-MHD, 10^{-10} density floor P and T-floor resets	EMEI-MHD, 10^{-6} density floor P and T-floor resets

80 ns

90 ns

100 ns

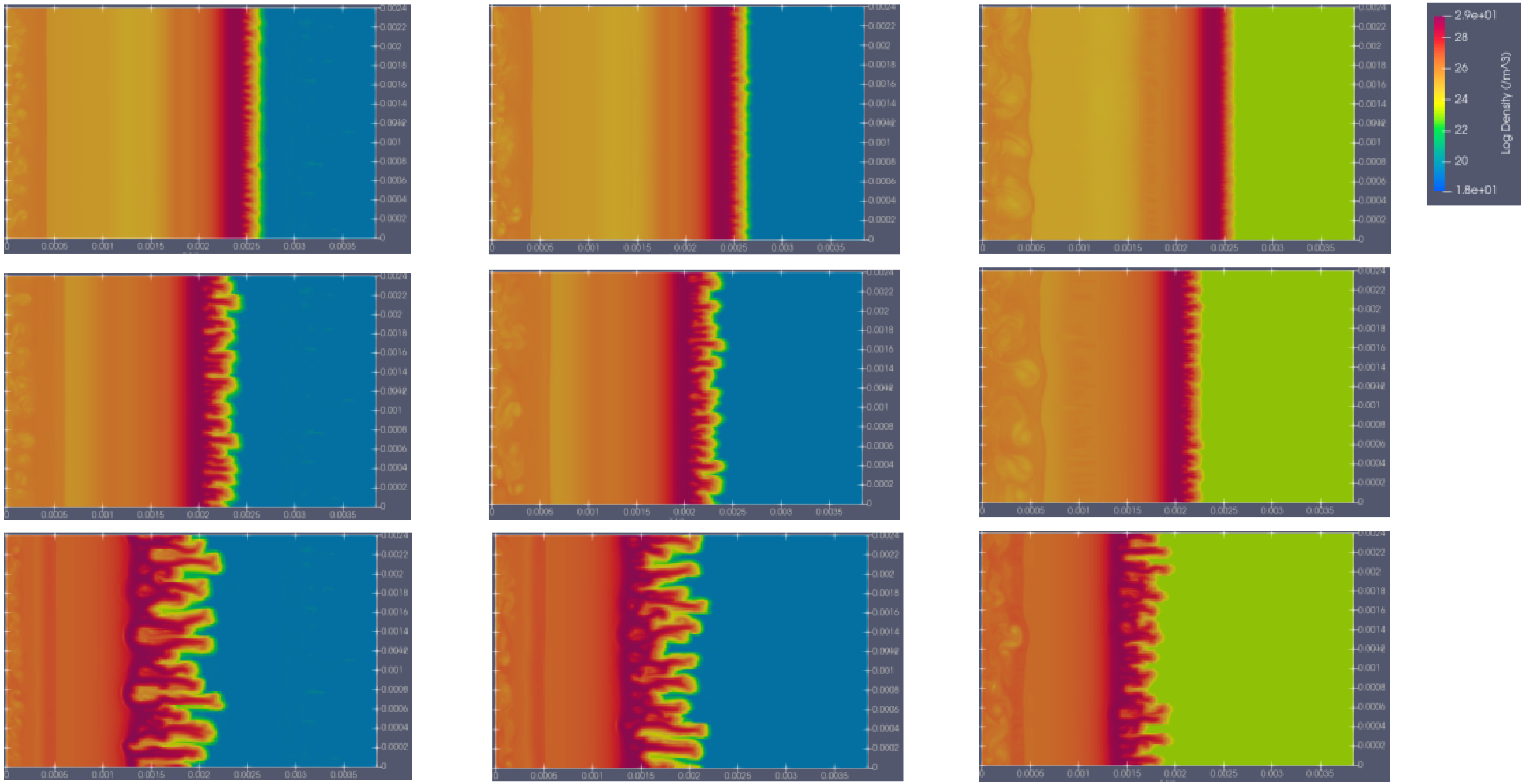

2-D MRT with sinusoidal outer surface

- Axisymmetric cylindrical geometry
- Initial temperature = 1130 K for Cu, 300 K for Be
- Initial pressure ~ 5×10^{-5} Torr
- Peak current = 26 MA
- $I(r_{max}, t) = I_{max}\sin^2\left(\frac{\pi t}{2\tau}\right)$
- 100-ns rise time:
- Domain: 3.84x2.4 mm, 192x120 cells
- Cell size = 20 microns
- Liner Parameters:
  - Initial density for Cu = 8960 kg/m^3
  - Initial density for Be = 1850 kg/m^3
  - Aspect ratio = 32
  - Outer radius = R_0 =2.88 mm
  - Inner radius = 2.79 mm
- MRT seed:
  - sinusoidal perturbation of outer liner radius at nodal resolution
  - Peak-to-valley = 160 microns
  - λ = 800 microns

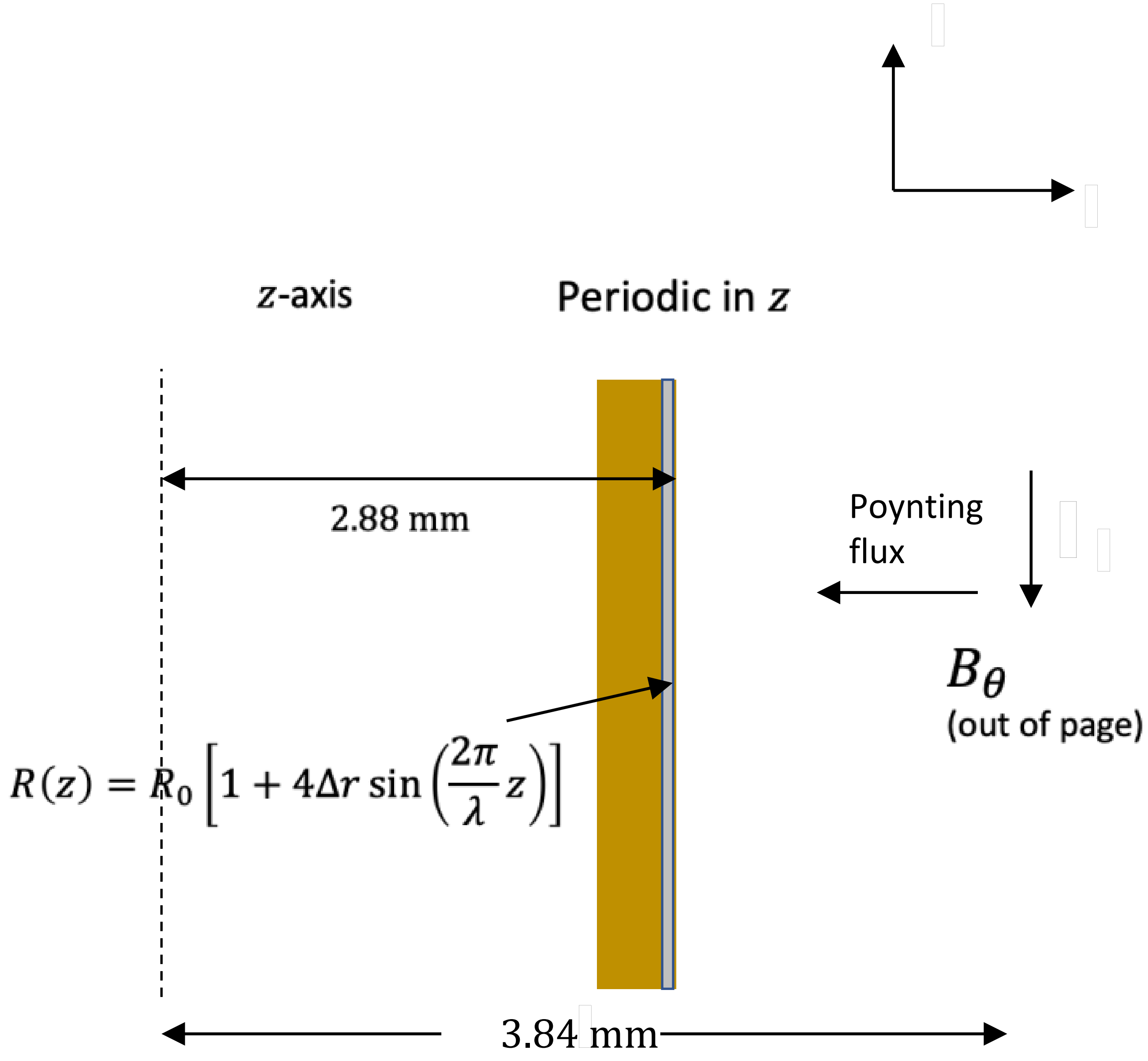

2-D MRT with Cu is consistent with analytic theory

Cu at 1130 K, EMEI-MHD,
$\rho_{floor} = 10^{-10}$ of solid Cu

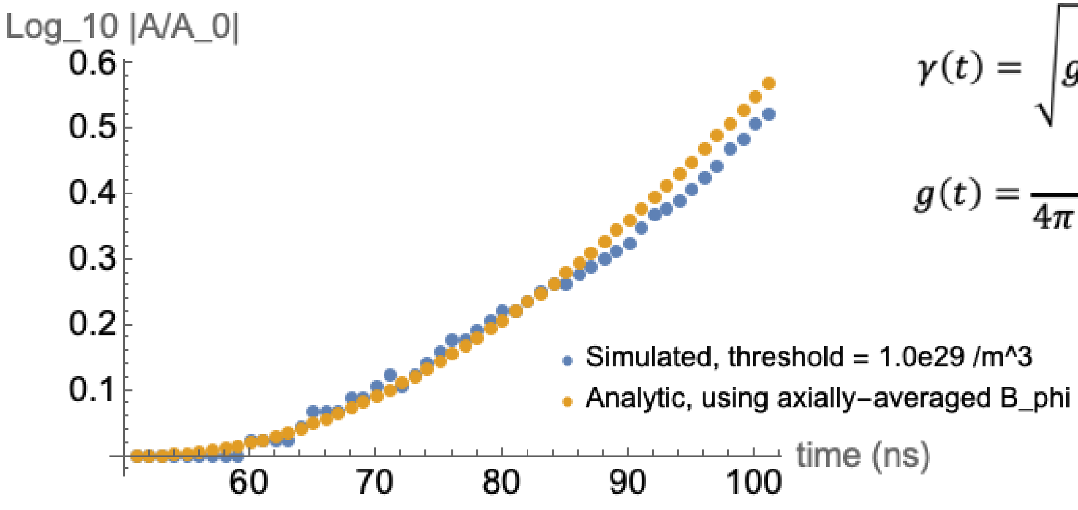

$$A(t) = A(t_0)\cosh\left[\int_{t0}^{t}\gamma(t')dt'\right]$$

$$\gamma(t) = \sqrt{g(t)\frac{2\pi}{\lambda(t)}}$$

$$g(t) = \frac{\mu_0 I(t)^2}{4\pi\ \rho\pi(r_{out}(t)^2\ - r_{in}(t)^2)\ r_{out}(t)}$$

$$I(t) = 2\pi\frac{r_{out}(t)}{\mu_0} < B_\phi >$$

$< B_\phi >$ is axially-averaged just outside liner..

Sinars et al, Phys. Plasmas, **18**, 056301, 2011
Weis et al, Phys. Plasmas, **22**, 032706, 2015

ALEGRA simulations also show secondary growth at this resolution (10 μm). (Gabe Shipley)

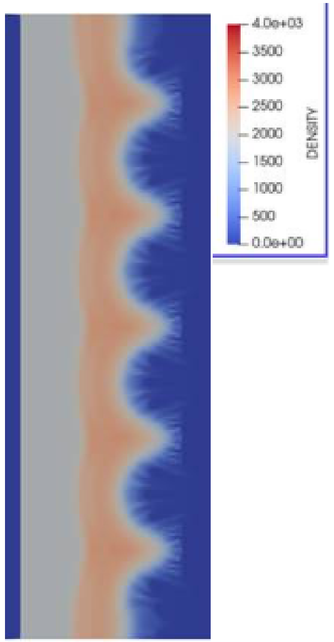

50 ns 60 ns 70 ns 85 ns 100 ns

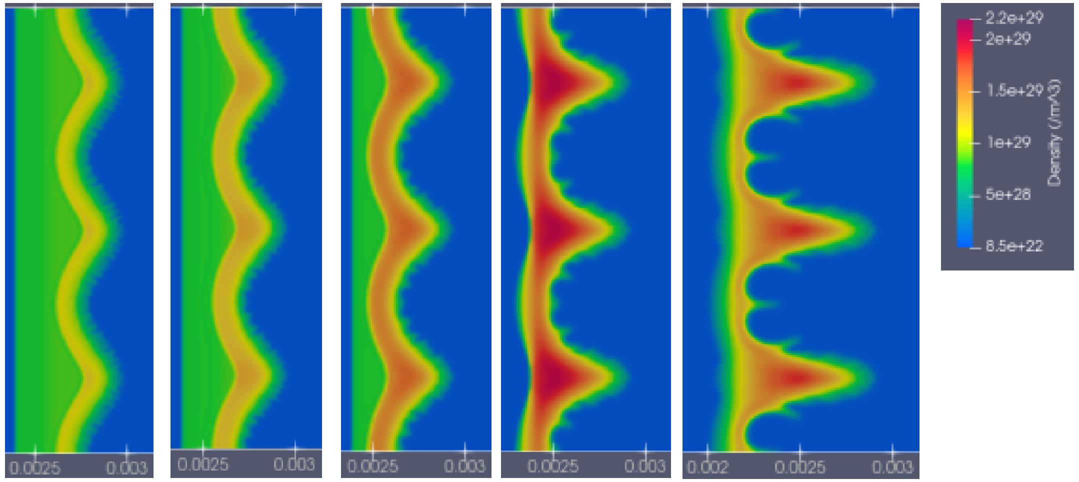

Wavelength = 800 μm

Lower density thresholds pick up secondary growth (probably ETI).

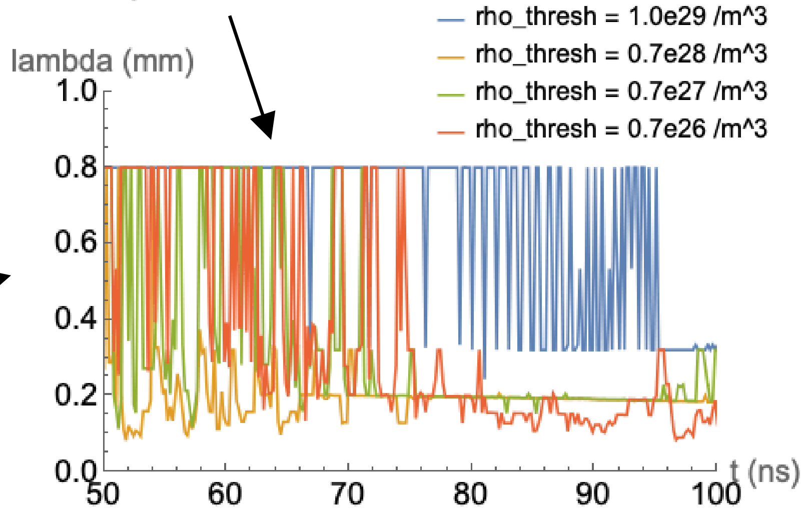

Secondary growth is damped out at coarser resolution

Be at 300 K, EMEI-MHD,
$\rho_{floor} = 10^{-6}$ of solid Be
Quadrature initialization

Secondary growth is captured at sufficient grid resolution.

- At coarse resolution, these high-frequency modes are damped out.

20-micron cell size
Wavelength = 1600 μm
Peak-to-valley = 320 μm

40-micron cell size
Wavelength = 1600 μm
Peak-to-valley = 320 μm

80-micron cell size
Wavelength = 3200 μm
Peak-to-valley = 640 μm

50 ns

50 ns

50 ns

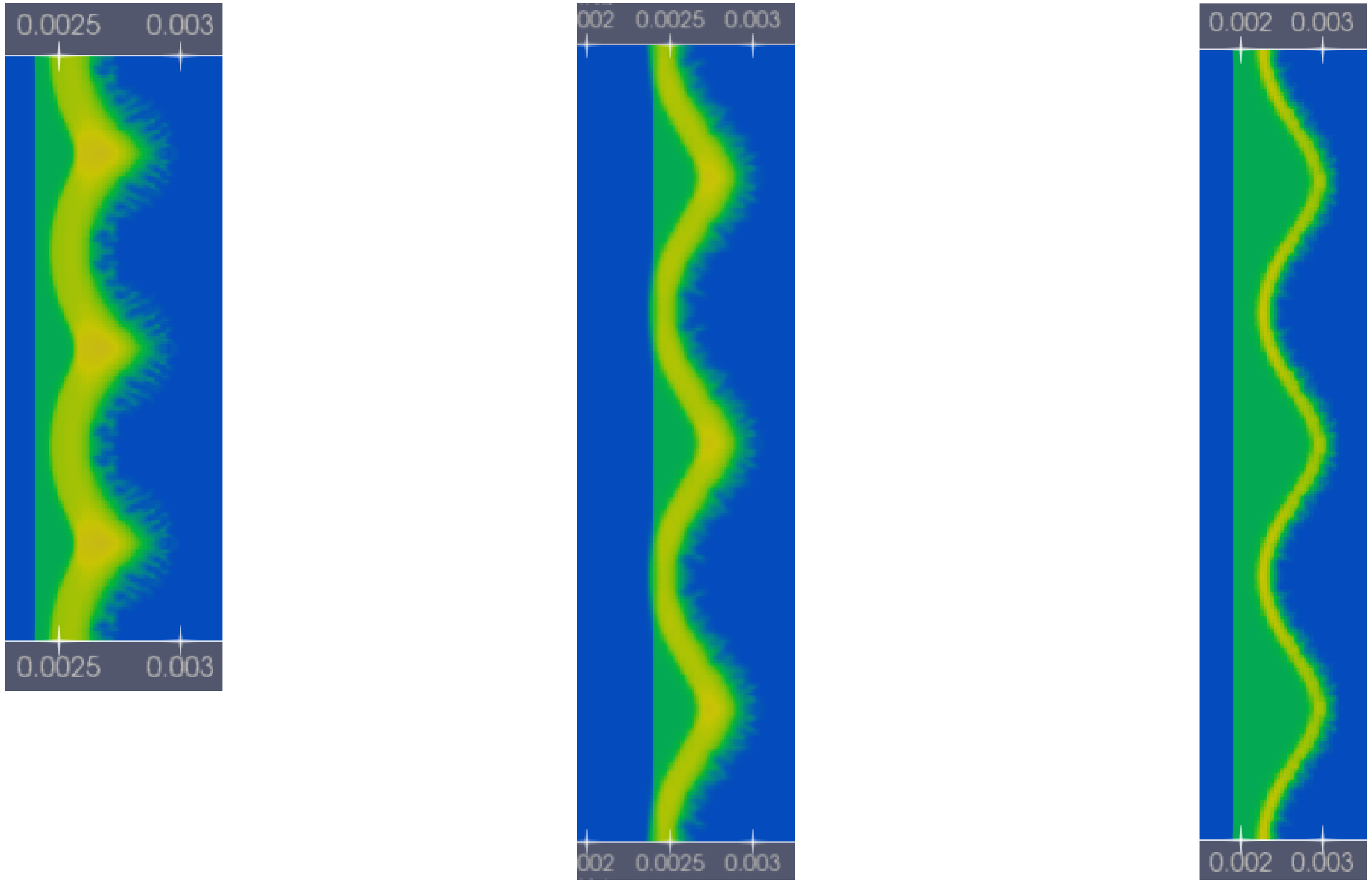

1-D Cu slab PERSEUS/HYDRA validation problem

- Cross-section of rod in slab geometry
- 600-cell domain spans $-6 \leq x \leq 6$ mm, so cell size = 20 microns
- Linear $\{1, x\}$ DG basis in each cell
- Rod extends over $-1 \leq x \leq 1$ mm
- Initial density = 8900 kg/m^3
- Initial temperature = floor temperature = 300 K
- Density floor = 1e-3 kg/m3
- EOS: Cu_3326_EOS (HYDRA was not able to use exactly this table.)
- Conductivity: CuV15_15Jul20.ses (HYDRA was not able to use exactly this table.)
- Periodic in y and z (only 1 cell needed in y and z)
- $B_y(6\text{ mm}, t) = B_{max}\sin^2\left(\frac{\pi t}{2\tau}\right)$, $B_{max} = 1000$ T
- $B_y(-6\text{ mm}, t) = -B_{max}\sin^2\left(\frac{\pi t}{2\tau}\right)$, $B_{max} = 1000$ T
- t_rise = $\tau = 100$ ns
- t_final = 2*t_rise $= 2\tau$

FLEXO and PERSEUS results are in close agreement.

- The tabular EOS and conductivity interface in FLEXO is working as expected.

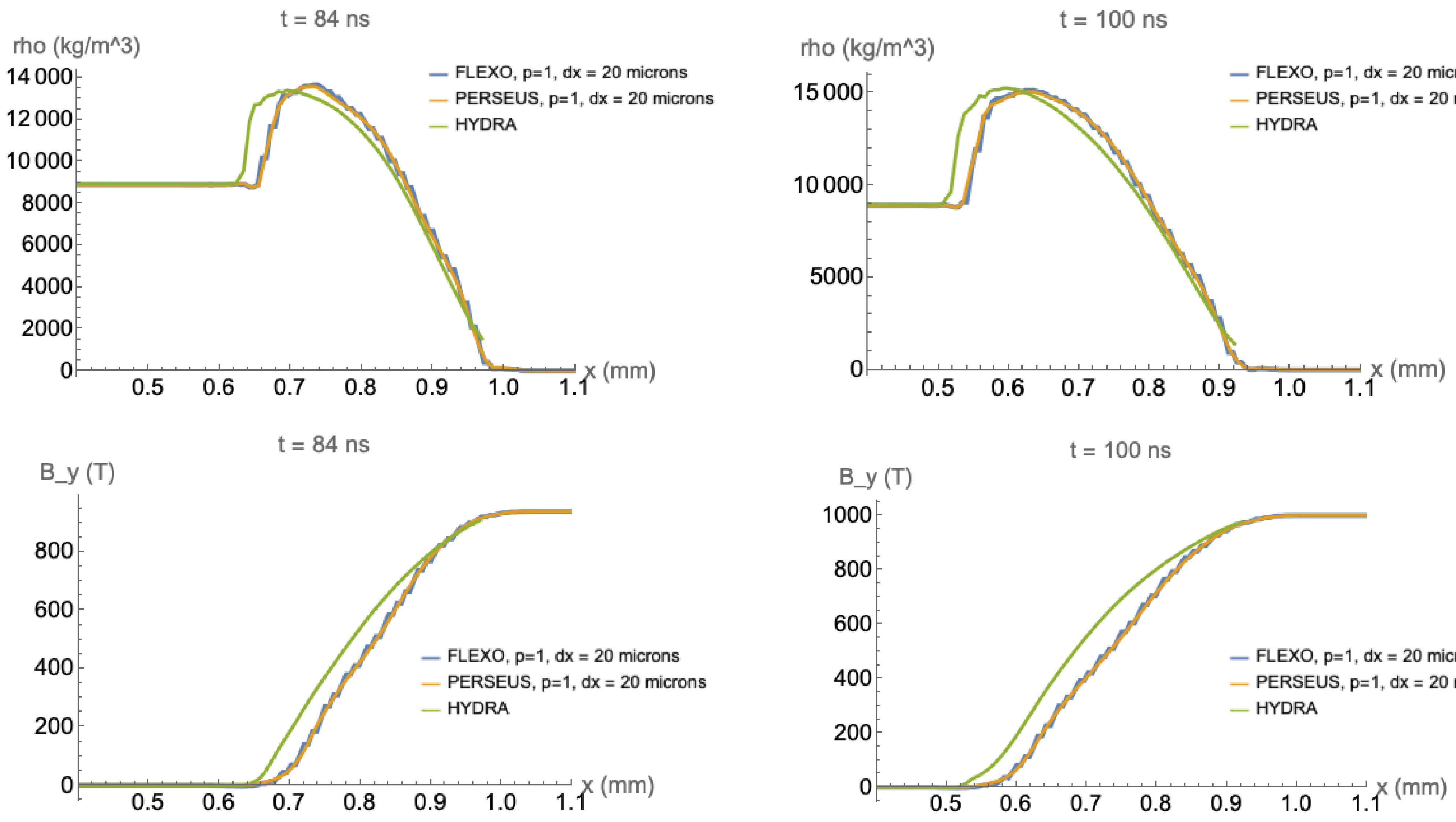

A Few Recent Successes in FLEXO

- B-field diffusion in FLEXO matches analytic solution in 1-D problem.
- FLEXO models the propagation of a 1-D Whistler wave at expected convergence rate, indicating correct modeling of Hall physics.
  - Inclusion of Hall term improves accuracy by 100X.
  - Added input flag for switching Hall term on and off.
- The FLEXO routines give the same interpolated tabular EOS and conductivity as PERSEUS for a set of representative densities and temperatures.
- FLEXO has a working tabular EOS and conductivity interface.
  - For PERSEUS/HYDRA 1-D slab validation problem, FLEXO and PERSEUS results are almost visually indistinguishable.
  - Uses positivity-preserving limiting by internal energy rather than pressure.

Conclusions/Summary

- A number of measures have enabled PERSEUS to simulate tabular EOS/conductivity at sufficiently low density floors to minimize dependence on vacuum/floor parameters:
  - Extended-range SESAME tables provided by Kyle Cochrane
  - Modeling of displacement current so Alfven speed is limited by the speed of light
  - Modeling of Hall physics via semi-implicit advance; no need to resolve Whistler wave and electron time scales
    - Minimal added CPU expense, since solve is local.
- Convergence w.r.t. density floor and vacuum parameters has been demonstrated in numerous test problems, including
  - 1-D target implosion; particularly evident in post-stagnation
  - 2-D MRT; growth rate not converged at density floors used by MHD codes
- Significance of minimizing floor sensitivity
  - More predictive model of energy coupling and target performance
  - Ability to simulate physical vacuum
  - Improved portability between experiments
    - Fewer artificial knobs to tune separately for each experiment.
- For MRT seeded by sinusoidal outer radius, linear MRT growth rate is consistent with analytic theory.
- Measures that tend to stabilize tabular interface
  - Bounds-preserving internal energy rather than pressure
    - 1-D tabular validation problem, particularly with extended-MHD
    - This should probably be an option in FLEXO.
  - Avoiding extrapolation

Thermal conduction implementation in PERSEUS

- Equations (thermal conduction in red):
  - $\frac{\partial \rho}{\partial t} + \nabla \cdot (\rho \boldsymbol{v}) = 0$
  - $\frac{\partial}{\partial t}(\rho \boldsymbol{v}) + \nabla \cdot (P\boldsymbol{I} + \rho \boldsymbol{v}\boldsymbol{v}) = \mathrm{J} \times B$
  - $\frac{\partial e_{tot}}{\partial t} + \nabla \cdot \left[(e_{tot} + P)\boldsymbol{v} - \kappa(q \cdot b)b - \kappa_{\perp}[q - (q \cdot b)b]\right] = (\boldsymbol{J} \times \boldsymbol{B}) \cdot \boldsymbol{v} + \eta J^2 \qquad \boldsymbol{b} = \boldsymbol{B}/B$
  - $\frac{\partial \boldsymbol{q}}{\partial t} - \nabla \mathrm{T} = -\nu \boldsymbol{q} \qquad \boldsymbol{\nu} \sim \mathbf{1/\Delta t}$
- Note that for $\nu \Delta t \gg 1$, $\boldsymbol{q}$ relaxes to ∇T. $\kappa(\rho, T)$ is computed by interpolation of SESAME κ sampled over ρ and T .
- The Lee-More-Desjarlais (LMD) model is currently being used for computing $\kappa_{\perp}$. This is the C-routine bfield_tcon_perp().
- In the nodal (quadrature) flux computation (left/right edge nodes for computing interface fluxes, and internal nodes for internal fluxes):
  1. $F_j(q_j) = T$ (At each node, T is computed from ρ and internal energy e_{int} by calling the ``reverse_interp" C-routine.)
  2. For each pair of nodes j_1 and j_2 in direction j, q_{j1} **and** q_{j2} must both have the same sign as $T_{j2} - T_{j1}$.
  3. **If** the above condition is satisfied, $F_j(e_{tot})$ is modified (see above equation) by $(\kappa \nabla T)_j = \kappa(q \cdot b)b_j + \kappa_{\perp}[q_j - (q \cdot b)b_j]$
- In the interface flux computation, the flux of q across an interface is computed using Local Lax-Friedrichs with wave speed $v_{\phi} = |v_j| + c_s$:
  - $F_j(q_j) = \frac{1}{2}[F_{j+}(q_j) + F_{j-}(q_j)] - \frac{1}{2} v_{\phi}(q_{j+} - q_{j-})$
- The density, momentum, and energy fluxes are still computed using the HLLC approximate Riemann solver.
- To advance q from timestep n to n+1, repeat the following for N sub-cycles (N usually = 5):
  - $q^* = q^m - \frac{\Delta t}{N} \nu \nabla T^n$
  - $q^{m+1} = \frac{q^*}{1 + \nu \Delta t / N}$
- After the above advance, compute the thermal conduction velocity:
  - $v_{TC} = \frac{\kappa q}{C_V T}$
- If v_{TC} exceeds the numerical speed of light c, then multiply each component of $\boldsymbol{q}$ by the factor v_{TC}/c and zero out the higher-order modes of $\boldsymbol{q}$.
- In the limiting, zero out the higher-order modes of q whenever the higher-order modes of momentum and current are zeroed out (e.g. when density falls to within a buffer region of the floor, or when internal energy falls below the minimum tabulated value).

Preliminary verification for step-function temperature initialization in solid slab

Solid Be slab
T_{hot} = 2000 K
T_{cold} = 300 K
κ = 1000 W/m/K
C_v = 50000 J/m³/K

Constant κ

Hydro turned off

$$\frac{\partial \epsilon}{\partial t} + \nabla \cdot (\kappa q) = 0$$

$$\frac{\partial q}{\partial t} - \nu \nabla T = -\nu q$$

$$\nu = \frac{1}{\Delta t}$$

$$^* = \quad + \Delta \quad \nabla$$

$$q^{n+1} = \frac{q^*}{1 + \nu \Delta t}$$

- Full hot region as opposed to symmetry BC.
- Boundaries at 1.2 mm instead of 0.6 mm.

Wave-speed for CFL: 10^5 m/s

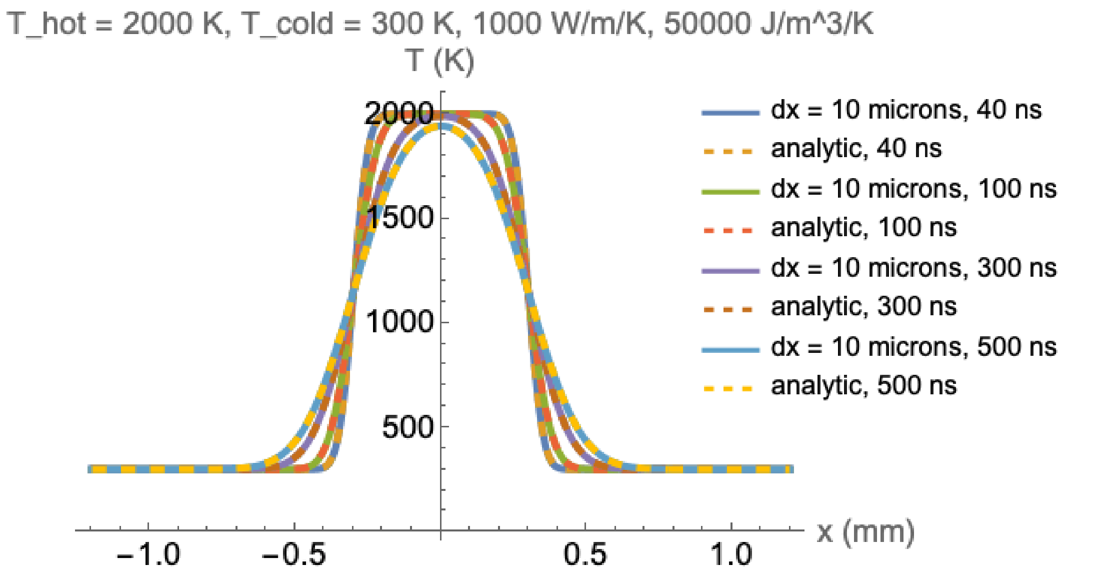

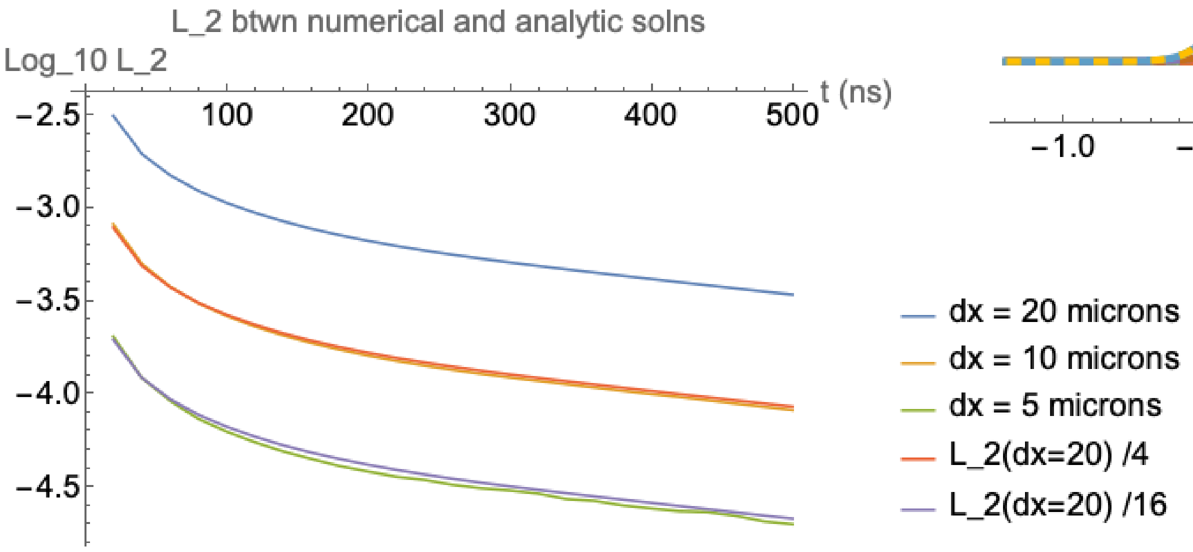

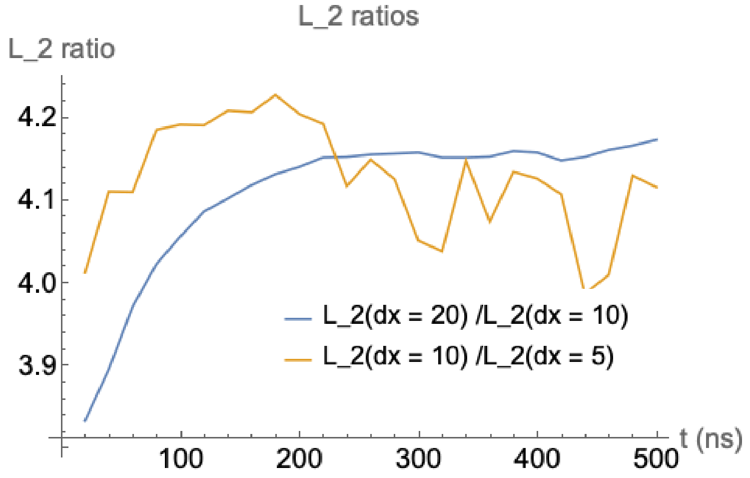

2021_1101_Tcond_1000d50000_5micron_1e5mps_2pt4mm

2021_1101_Tcond_1000d50000_10micron_1e5mps_2pt4mm

2021_1101_Tcond_1000d50000_20micron_1e5mps_2pt4mm

Preliminary verification of steady-state for solid slab heated at constant rate with fixed-temperature BCs :

- Dirichlet BCs
- constant energy source

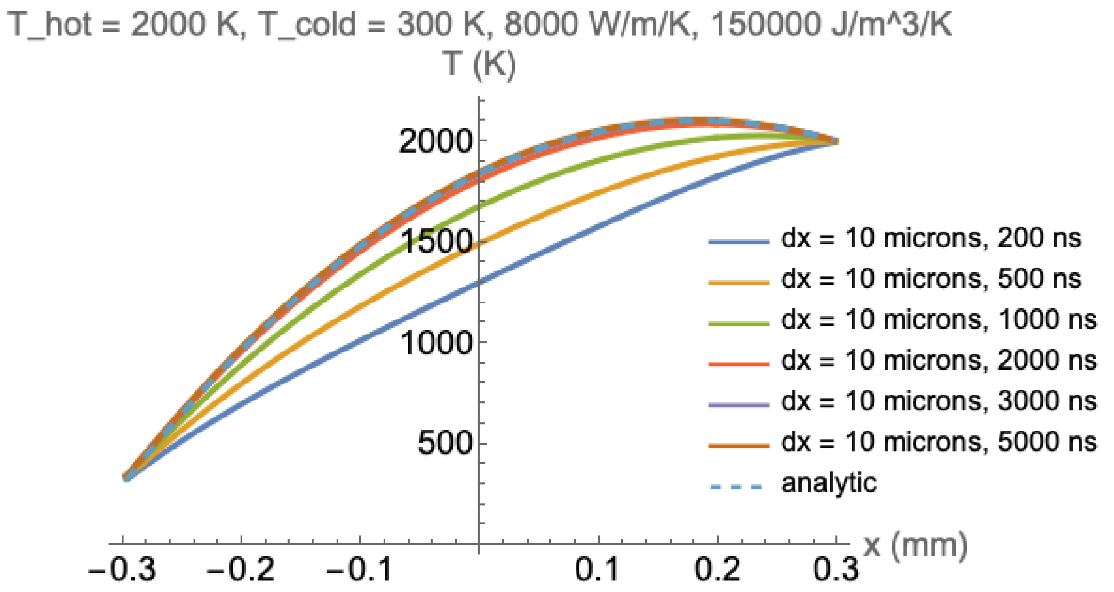

From Toptan et al, 2020,
https://asmedigitalcollection.asme.org/verification/article/5/4/041002/1090520/Construction-of-a-Code-Verification-Matrix-for

Solid Be slab
$L = 0.6$ mm
$x = -L/2$: T_{cold} = 300 K
$x = L/2$: T_{hot} = 2000 K

κ = 8000 W/m/K
C_v = 150000 J/m³/K
$$\tau = \frac{(0.6L)^2 C_v}{\kappa}$$
$$P_T = \frac{2000\ \mathrm{K}}{\tau}$$

Initialized with linear temperature profile.

Analytic steady-state profile:

$$T(x) = T_{cold} + (T_{hot} - T_{cold})\frac{x}{L} + \frac{P_T}{2\kappa/C_v}x(L - x)$$

Thermal conduction model:

$$\frac{\partial \epsilon}{\partial t} + \nabla \cdot (\kappa q) = C_v P_T \qquad \frac{\partial q}{\partial t} - \nu \nabla T = -\nu q \qquad \nu = \frac{1}{\Delta t}$$

$$^* = \quad + \Delta \quad \nabla$$

$$q^{n+1} = \frac{q^*}{1 + \nu \Delta t}$$

2021_1020_slab01_10micron_1e5mps

2021_1020_slab01_20micron_1e5mps